AIAA JOURNAL
Vol. 30, No. 6, June 1992

Effect of Acoustic Excitation on Stalled Flows over an Airfoil

K. B. M. Q. Zaman*
NASA Lewis Research Center, Cleveland, Ohio 44135

The effect of acoustic excitation on poststalled flows over an airfoil, i.e., flows that are fully separated from near the leading edge, is investigated. The excitation results in a tendency toward reattachment, which is accompanied by an increased lift and reduced drag, although the flow may still remain fully separated. It is found that, with increasing excitation amplitude, the effect becomes more pronounced but shifts to a Strouhal number that is much lower than that expected from linear, inviscid instability of the separated shear layer.

Nomenclature

C_l	= lift coefficient
c	= chord of airfoil
f_{opt}	= approximate value of f_p producing optimum increase in lift
f_p	= excitation frequency
R_c	= chord Reynolds number, $U_\infty c/\nu$
St	= Strouhal number, $f_p c/U_\infty$; $St_{opt} = f_{opt} c/U_\infty$
S_u	= one-dimensional spectrum of $\langle u' \rangle$
$\langle U \rangle$	= mean velocity measured with a single hot wire approximating $(U^2 + V^2)^{1/2}$
U, V	= mean velocities in x,y directions, respectively
$\langle U_m \rangle$	= maximum $\langle U \rangle$ just outside the boundary layer
U_∞	= freestream U
$\langle u' \rangle, \langle u'_f \rangle$	= rms total and fundamental fluctuation in the direction of $\langle U \rangle$, as measured by a single hot wire
$\langle u'_r \rangle$	= $(u'^2_r + v'^2_r)^{1/2}$
u', v', w'	= rms velocity fluctuations in x,y,z directions, respectively
x'	= streamwise distance from leading edge
x,y,z	= streamwise, transverse, and spanwise coordinates, respectively
y'	= transverse distance from airfoil surface
α	= angle of attack
θ	= momentum thickness

Subscript

r	= values at reference location

I. Introduction

THE effect of acoustic excitation on flow separation over airfoils has been studied previously by several investigators.[1-12] In Ref. 10, the general effect over a large α range was investigated, addressing such questions as the roles of the tunnel resonance and the instability of the boundary layer in the process. Differences were observed in the effect depending on the α range. At low α, laminar boundary layer separation occurred—a condition that aggravated with decreasing chord Reynolds number R_c. It was found, subsequently,[12] that the laminar separation could be effectively reduced by a small amplitude excitation, within the R_c range covered (2.5×10^4–10^5), when the parameter $St_{opt}/R_c^{1/2}$ fell in the range 0.02–0.03. For this case, the optimum effect apparently occurred when the excitation frequency matched the instability frequency of the separated shear layer. Around the onset of static stall ($\alpha \approx 15$ deg) for the airfoil under consideration, a transitory stall occurred at an unusually low frequency.[11] The effect of acoustic excitation on this phenomenon was rather complex, and depending on the range of f_p, the low frequency oscillation could either be augmented or suppressed. The excitation under certain conditions for this case actually decreased the lift coefficient. In comparison, the excitation at large α, i.e., in the poststalled case, consistently increased the C_l, but the effect was noted to be strongly dependent on the excitation amplitude.[2,10]

In the present paper, excitation effect on the poststalled flows is considered. As indicated earlier, these flows are defined as ones that are fully stalled, i.e., fully separated from near the leading edge. In contrast to the laminar separation, the separated shear layer in this case undergoes transition to turbulence while still over the airfoil, or at sufficiently high R_c, the separating boundary layer may already be turbulent. However, the angle of attack is large enough so that even the turbulent shear layer cannot reattach.

Most previous excitation studies concerned the poststall situation. A review reveals an interesting anomaly among the published results. With reference to Table 1, the Strouhal number St_{opt} based on the effective excitation frequency f_{opt} is found to vary widely from experiment to experiment. (In most of these studies the excitation effect for limited values of f_p was reported and f_{opt} was not determined rigorously. Typical examples from these studies are listed in Table 1. For the present comparison, it is reasonable to assume that the values of f_p producing a large effect in these examples represented f_{opt}.) Note that between Refs. 3 and 8, for similar α, R_c, and airfoil, there is an order of magnitude difference in St_{opt}. Between Refs. 9 and 10, the results may be extrapolated to yield an even larger difference in St_{opt} for comparable R_c. Here, one could reason that f_{opt} should scale on the separated shear-layer momentum thickness (θ), and thus, whereas St_{opt} might vary, a nondimensional frequency based on θ (i.e., $f_{opt}\theta/U_\infty$) would be expected to remain a constant. However, the results in Table 1 would then suggest order(s) of magnitude difference in θ for comparable flows. Even though these experiments are done in different wind tunnels, this is highly unlikely. For comparable airfoils at comparable U_∞, θ for the separated shear layer immediately downstream of the leading edge must be close in magnitude. Thus, a large difference in St_{opt} also implies a large difference in the nondimensional frequency based on θ.

From Table 1, it is apparent that "external" excitation produces the effect at high St, whereas "internal" excitation

Presented as Paper 90-4009 at the AIAA 13th Aeroacoustics Conference, Tallahassee, FL, Oct. 22-24, 1990; received Feb. 4, 1991; revision received Sept. 4, 1991; accepted for publication Sept. 9, 1991.

*Aerospace Engineer, Mail Stop 5-11. Senior Member AIAA.

Table 1 Excitation parameters from previous studies

Reference	Airfoil	α, deg	$R_c \times 10^{-5}$	St_{opt}	Excitation type
Collins and Zelenevitz[1]	NACA 2412	20–24	5.3	28–94	External
Ahuja and Burrin[2]	—	16	5	2.7	External
Marchman et al.[3]	Wortmann	15	2	27	External
Neuburger and Wygnanski[8]	Wortmann	16	2	1.8	Internal vibrating ribbon
Hsiao et al.[7]	NACA 63-018	18–24	0.2–3	≈ 2	Internal acoustic
Huang et al.[6]	—	15–20	0.35	≈ 1	Internal acoustic
Nishioka et al.[5]	Flat plate	8–14	0.4	3.8–27	External
Bar-Sever[9]	LRN	20	1.5	1.5	Internal vibrating wire
Zaman et al.[10]	LRN	18–22	0.4–1	7–40	External

is effective at lower St. An exception is the result of Ref. 2. External excitation typically involves acoustic irradiation with a source away from the airfoil.[1-5,10-12] Internal excitation, on the other hand, involves direct introduction of velocity perturbations in the flow, e.g., acoustically through slots on the airfoil[5,7] by vibrating ribbon[8] or by a vibrating wire placed near the leading edge.[9] In general, a more profound effect was observed using internal excitation.

The question that arises naturally is, What is the difference between the two methods that produces the effect in such different ranges of St? In both cases, the perturbation has to act on the instability of the separating boundary layer. Nishioka et al.[5] eloquently said, "The instability of the separated shear layer is quintessential as the underlying mechanism which enables the sound waves to suppress the separation." However, linear, inviscid instability of the separated shear layer may not be expected to govern the effect of the excitation in the poststall flows. The instability mechanism responsible for the effect in this case must be complex due to nonlinearity associated with the high amplitudes, as well as due to the presence of the wall. In fact, the main result of the present experimental investigation is an amplitude dependence of the excitation effect. It will be shown that with increasing amplitude the effect becomes very pronounced but shifts to a lower St, which, although remaining unexplained from flow instability considerations, reconciles the anomaly noted earlier. The amplitude dependence also reconciles the difference between the results of external and internal excitation, as the latter technique apparently introduces larger-amplitude perturbations.

In the present study, external excitation is used in which the amplitude is varied in a controlled manner within the constraints of the tunnel resonances. Parametric dependence of the excitation effect on frequency and amplitude is studied for three Reynolds numbers. The flowfield for a specific large amplitude excitation case is then documented in detail.

II. Experimental Facility

The experiments were carried out in the NASA Lewis low-speed wind tunnel, which has been described in detail in Refs. 11 and 12. The schematic of the test section is shown in Fig. 1. The maximum tunnel speed is about 12 m/s with a freestream turbulence intensity less than 0.1%. A two-dimensional airfoil [LRN (1)-1007] with chord $c = 12.7$ cm and aspect ratio of 6 is used in the experiment; the cross-sectional shape of the airfoil is shown by the inset in Fig. 2. Two acoustic drivers and a 40.6-cm woofer are used for excitation, covering a wide frequency range from 15 Hz to 15 kHz. Only one speaker is used at a time; for $f_p < 700$ Hz, the woofer is used, for $f_p > 700$ Hz, one of the acoustic drivers is used. A crossed hot-film probe (DISA 55R53) is used to measure velocity fluctuation amplitudes u' and v', at a reference location about $0.4c$ upstream of the airfoil leading edge. The resultant of u' and

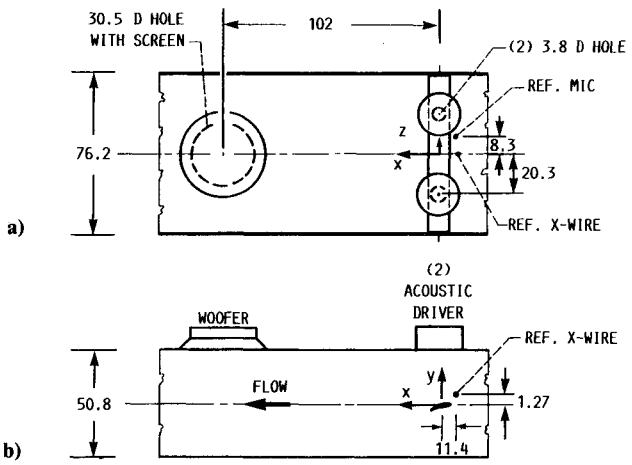

Fig. 1 Schematic of wind-tunnel test section; dimensions are in centimeters: a) top view; b) front view.

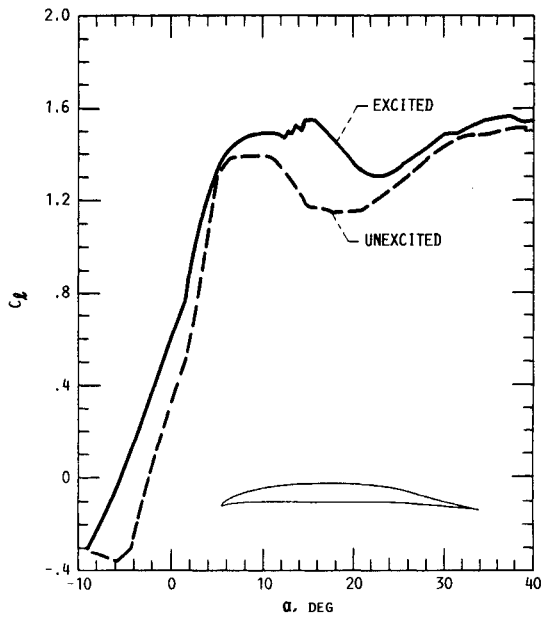

Fig. 2 C_l vs α with and without excitation: excitation at $f_p = 342$ Hz, $\langle u_r' \rangle / U_\infty = 1.5\%$; $R_c = 7.5 \times 10^4$.

v' measured at this fixed location is denoted as the reference amplitude parameter $\langle u'_r \rangle$, which is expressed as percentage of U_∞. A computer controlled traversing mechanism is used to move a single hot wire to measure the velocity field around the airfoil. The coordinate origin is at the tunnel midheight ($y = 0$) and midspan ($z = 0$) and at the airfoil midchord ($x = 0$).

For convenience, the streamwise coordinate x' for some data has been referenced to the airfoil leading edge. Lift is measured by a balance mechanism. For further details of the experimental procedure the reader may consult Refs. 11 and 12.

III. Results and Discussion

A. Amplitude Effect

First, let us briefly review the essential features of the tunnel resonance characteristics, which have been discussed in detail in Ref. 12. At low f_p, longitudinal resonances are encountered. At these resonance conditions, for $f_p \lesssim 280$ Hz, primarily u' fluctuations are induced, which are uniform over the tunnel cross section at a given x station. With increasing f_p, increasingly complex resonances occur, which are characterized by nonuniform amplitude distributions over a given cross section of the tunnel. However, well-defined excitation conditions can be achieved at certain higher f_p. One such case is the fundamental cross resonance at 342 Hz, which is characterized by an antinode in velocity perturbation at the tunnel midheight. Large v', uniform in the spanwise direction, is induced at this f_p in the vicinity of the airfoil. Because of the availability of large amplitudes, some detailed measurements were conducted at this f_p. Similarly, large-amplitude perturbations, uniform in z, can also be induced at even higher f_p, e.g., at the odd harmonics of 342 Hz. However, achieving a two-dimensional perturbation field becomes increasingly difficult with increasing f_p.

Figure 2 shows the lift coefficient C_l variation with the angle of attack α with and without excitation at 342 Hz. The amplitude of excitation is large, and the lift is found to increase over the entire α range covered. For the flow under consideration, the low frequency transitory stall is induced by the excitation approximately in the α range of 14–16 deg; this is accompanied by an unusual increase in the C_l.[11] However, in this paper, the excitation effect is studied for the fully stalled condition that occurs in the range $\alpha \geq 16$ deg.

The excitation amplitude effect is shown for several α in Fig. 3. Large gains are achieved at the lower α, but the effect diminishes with increasing α. Nevertheless, a perceptible increase in C_l occurs even at $\alpha = 30$ deg. Note the saturation and the subsequent breakdown in C_l with increasing amplitude in the range $16 < \alpha < 20$ deg. This aspect will be further addressed in Sec. III.C.

For $\alpha = 18$ deg, C_l vs $\langle u_r' \rangle$ was measured for a large number of f_p at a fixed R_c. Sample results are shown in Fig. 4 for three values of R_c. The Strouhal number St corresponding to each curve is indicated. Several of the curves are terminated on the right by the limitation in the available amplitude from the loudspeaker in use. Inspection should reveal that for constant amplitude at a given St, comparable gains are achieved at all three R_c.

The variations of C_l with St are cross plotted from data similar to those in Fig. 4 in Figs. 5a–c for the three R_c. These are hand smoothed curves through the data, and some of the

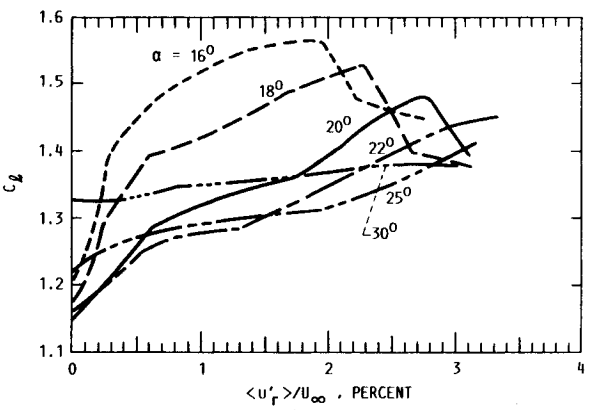

Fig. 3 C_l vs $\langle u_r' \rangle / U_\infty$ **for different** α: $f_p = 342$ **Hz,** $R_c = 7.5 \times 10^4$.

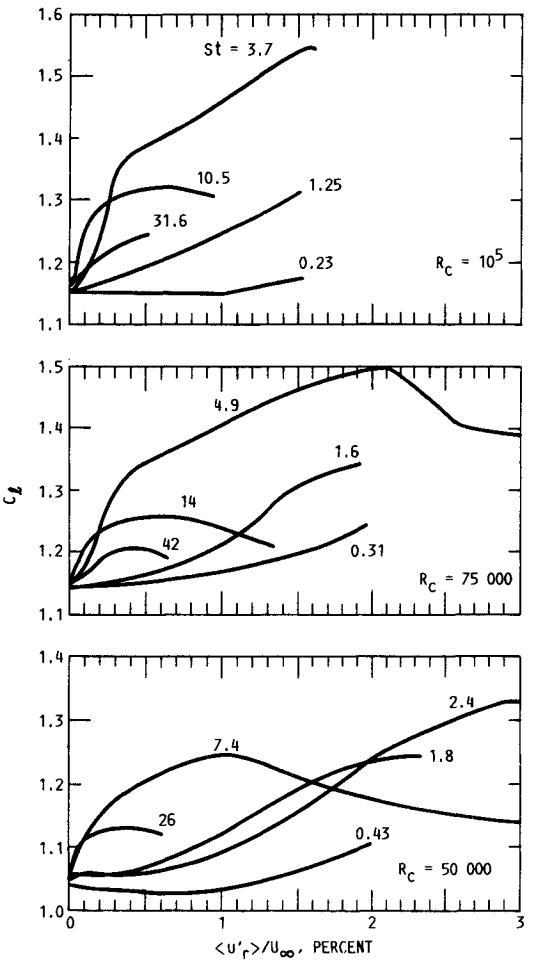

Fig. 4 C_l vs $\langle u_r' \rangle / U_\infty$ **for different** St. **The three sets of data are for indicated values of** R_c.

curves at high amplitudes are based on only three data points. However, it is clear that with increasing amplitude a large increase in C_l occurs but the effect shifts progressively to a lower St.

Over the amplitude range covered, the optimum increase in C_l is found to occur in the range $2 \lesssim St \lesssim 5$. One could speculate that, with even higher amplitudes of excitation, further increase in C_l could be achieved but it would occur at an even lower St, perhaps on the order of unity. For the flows studied, e.g., at $R_c = 7.5 \times 10^4$, the St range of 2–5 is substantially lower than the corresponding range for the linear, inviscid instability of the separated shear layer. The latter range can be inferred from hot-wire surveys near the leading edge. The time trace of u fluctuation in Fig. 6a shows a high-frequency periodicity superimposed on the low-frequency fluctuations. The high-frequency fluctuation characterizes the u' spectrum by a broadband hump centered around 2 kHz, as shown in Fig. 6b. This represents the (Kelvin-Helmholtz) instability frequency of the separated shear layer for the flow under consideration. Although there is subjectiveness, this is a simple way to experimentally determine the range of the shear-layer instability frequency; a similar method was also used in Refs. 6 and 13. The momentum thickness θ of the separated shear layer at $x'/c = 0.03$ was measured to be 0.07 mm. The frequency 2 kHz thus corresponds to a nondimensional value, $f\theta/U_\infty \approx 0.016$. This agrees with stability predictions for maximally amplified disturbances in a zero pressure gradient shear layer. (As discussed later, the pressure gradient in the separated, unexcited flow is indeed small.) Thus, the data confirm that the spectral hump around 2 kHz is due to the initial shear layer instability. Referring back to Fig. 5b, one finds that 2 kHz corresponds to $St \approx 30$ (indicated by the arrow) in contrast to

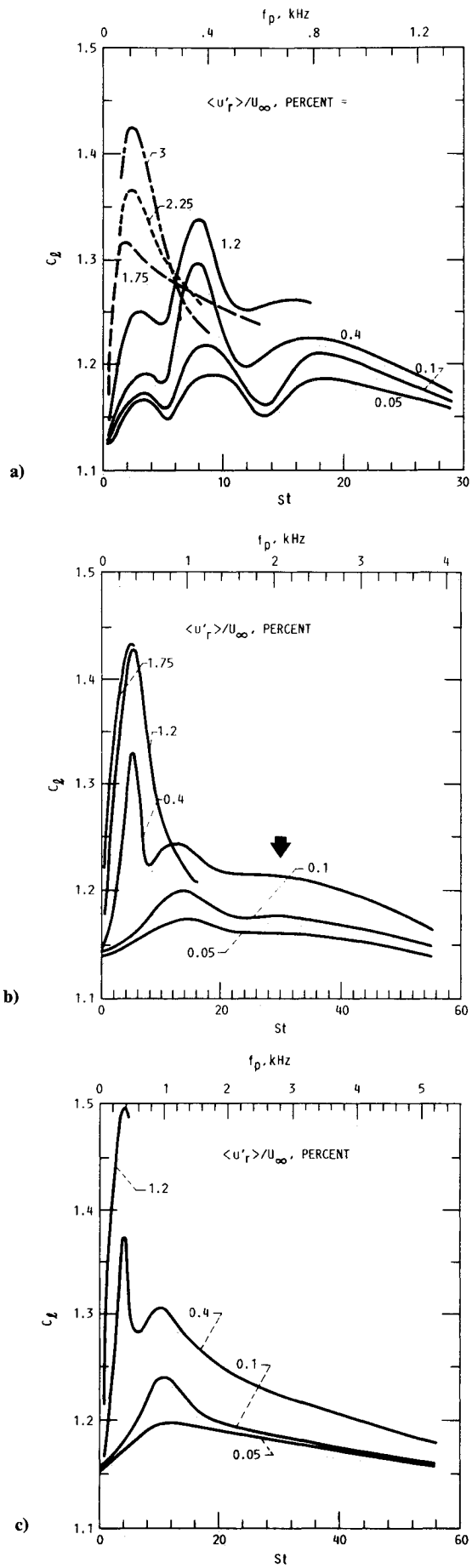

Fig. 5 C_l vs St for different $\langle u'_r \rangle / U_\infty$: a) $R_c = 5 \times 10^4$; b) $R_c = 7.5 \times 10^4$; and c) $R_c = 10^5$.

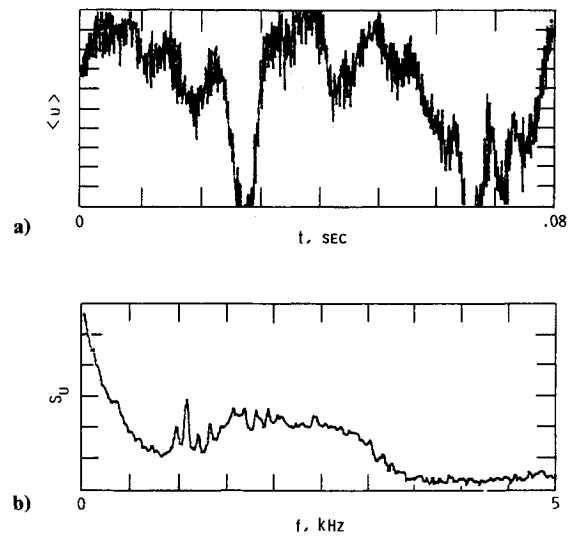

Fig. 6 $\langle u \rangle$ fluctuations near the high speed edge of the boundary layer at $x'/c = 0.03$; $\alpha = 18$ deg, $R_c = 7.5 \times 10^4$, no excitation: a) sample time trace; b) time-averaged spectrum.

the value $St \approx 4$ producing the optimum effect. Obviously, for $R_c = 10^5$ in Fig. 5c, this difference is even larger. In Ref. 13, which dealt with the excitation effect on the separation bubble over the blunt end of a cylinder placed parallel to the flow, a similar observation was made. As will be discussed further in Sec. IV, the excitation was found to be effective when the forcing frequency was much lower than the Kelvin-Helmholtz instability frequency of the initial shear layer. A similar trend was also observed in Ref. 5 for the flow over a flat-plate model at large α. Thus, the linear instability of the separated shear layer does not appear to be the primary mechanism through which the optimum excitation effect is achieved. Apparently, nonlinear effects play a significant role. Viscous effects could also be important as there is indication of a separation bubble near the leading edge (Sec. III.C). No analysis is presently available to address the observed effects satisfactorily.

The shift of the optimum effect to lower St with increasing amplitude should explain the anomaly discussed in Sec. I. With external excitation, typically, lower amplitudes are induced. For example, in Refs. 1 and 10, it is estimated from the sound pressure level data that approximately 0.1% amplitudes, in terms of the present notation ($\langle u'_r \rangle / U_\infty$), were used. One can roughly estimate the amplitude to be close to 2% in Ref. 2 for the data shown in Table 1. Thus, the large effect at low St observed in Ref. 2 agrees with the data trend found in the present experiment. For the internal excitation cases, none of the references clearly provide velocity amplitude data, but it is reasonable to assume that they are large.

B. Flowfield Detail

In the following, flowfield data are presented for excitation at $R_c = 7.5 \times 10^4$, with $f_p = 342$ Hz and $\langle u'_r \rangle / U_\infty = 1.5\%$. Mean velocity profiles measured at different chordwise locations on the upper surface are shown in Fig. 7. These data were measured with a single hot wire and there are errors due to hotwire rectification in regions of reverse flow near the wall. In the range where $\langle U \rangle / \langle U_m \rangle < 0.5$, the data have been corrected by an algorithm, which is chosen to approximate the probability distribution of reverse flow in comparable flowfields.[14] The correction function $g(y)$ is defined as,

$$\langle U_{\text{corrected}} \rangle = \langle U_{\text{measured}} \rangle * [1 - 2g(y')]$$

$$g(y') = 1 - 1/(1 + \exp\{2 * [(y'_{0.5} - y')/y'_{0.5} * 4 - 2]\})$$

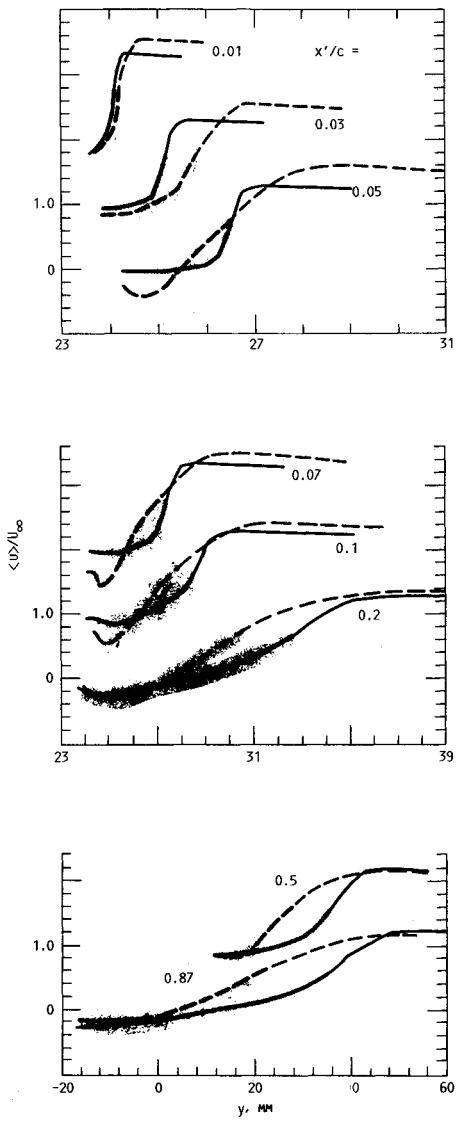

Fig. 7 Boundary layer profiles of $\langle U \rangle$ at different x'/c. Solid lines for unexcited flow, dashed lines for excitation with $f_p = 342$ Hz and $\langle u_f' \rangle / U_\infty = 1.5\%$; $\alpha = 18$ deg, $R_c = 7.5 \times 10^4$. In each set, ordinate pertains to lowest pair and other pairs are staggered by one major division.

so that $g(0) \approx 1$ and $g(y_{0.5}') \approx 0$. However, in the range where the correction is done (indicated by the shaded regions), the data should be considered only as qualitative. The composite plot of Fig. 7 provides a perspective on the effect of the excitation over the entire upper surface.

The corresponding rms fluctuation intensity profiles are shown in Fig. 8. (The profiles are staggered similarly as in Fig. 7, and the data corresponding to the shaded regions of Fig. 7 should be considered as qualitative.) In both Figs. 7 and 8, the boundary layer is found to thicken near the leading edge under the excitation. But downstream of $x'/c \approx 0.1$, the effect of the excitation is to reduce the transverse extent of the separated region.

The loci of the $0.7\langle U_m \rangle$ point with and without excitation, derived from several profiles similar to those in Fig. 7, are shown in Fig. 9a. The corresponding distributions of $\langle U_m \rangle$ for the upper shear layer only, are shown in Fig. 9b. The reduction in the separated region under the excitation and the accompanying change in the $\langle U_m \rangle$ distribution (and thus in the static pressure distribution) are clearly evident from these data. With reference to the discussion of Fig. 6, note that $\langle U_m \rangle$ is practically constant shortly downstream of the leading edge, thus indicating a near zero pressure gradient for the separated flow in the unexcited case.

It was noted in Fig. 8 that the fundamental rms amplitude becomes very small downstream of $x'/c \approx 0.2$. The amplitude $\langle u_f' \rangle$ (at 342 Hz) was measured along the $0.7\langle U_m \rangle$ points and is shown in Fig. 9c. These data approximately represent the $\langle u_f' \rangle$-maxima distribution. It is clear from the data for the upper shear layer that the amplitude becomes very large shortly downstream of the leading edge. The peak occurs at about the 3% chord location. But immediately downstream, the flow breaks down into turbulence, obliterating the fundamental. The following point may be made based on these data. Recall that the initial shear layer instability corresponds to $St \approx 30$, whereas the optimum effect takes place at an order of magnitude lower St (Fig. 5b). One could hypothesize that the large effect at the low St should be due to an effective excitation of the thicker shear layer downstream of the leading edge. This seemed plausible based on the knowledge of excitation

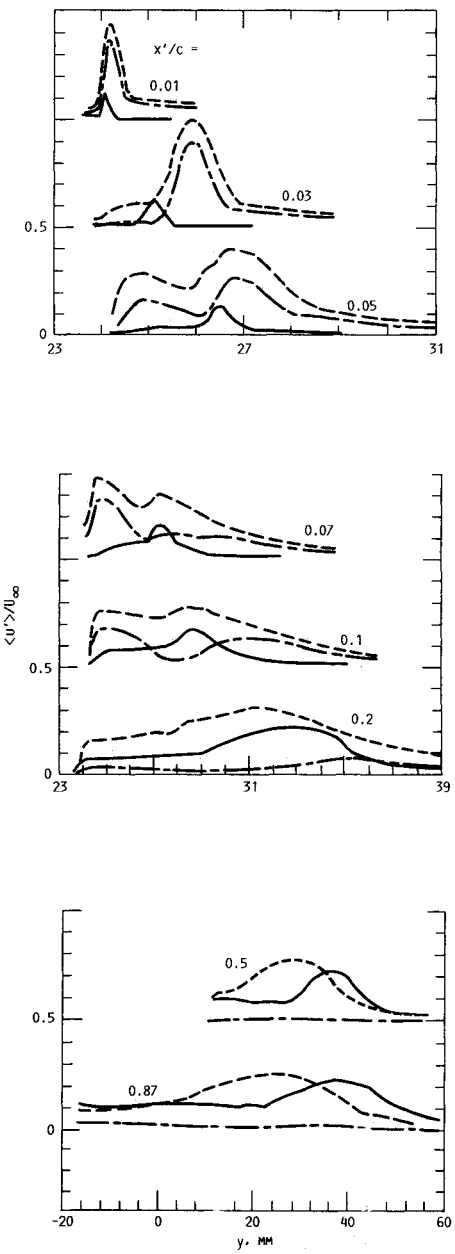

Fig. 8 Rms fluctuation intensity profiles corresponding to the data of Fig. 7. Solid line, unexcited flow; dashed line, for excitation. Chain-dashed lines for fundamental rms amplitude.

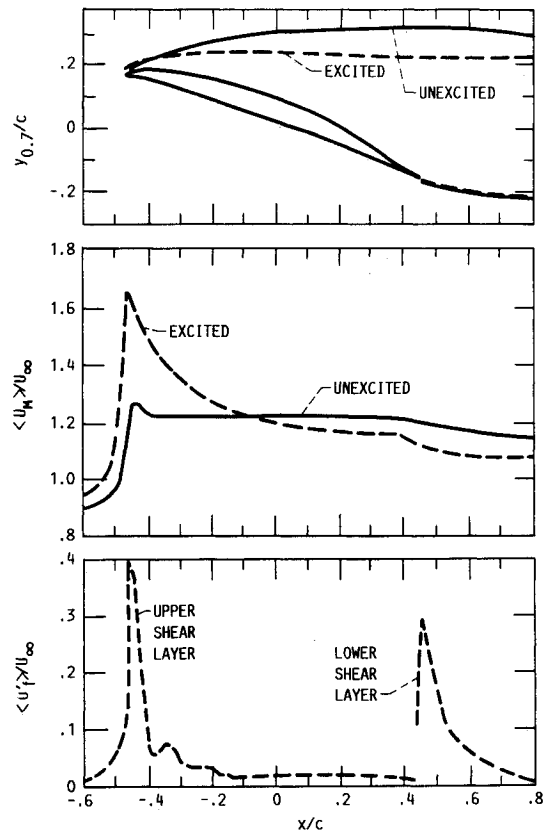

Fig. 9 Time-averaged mean and fluctuating velocity fields on the suction surface; same flow and excitation condition as in Fig. 7: a) loci of 0.7 $\langle U_m \rangle$ points; b) distribution of $\langle U_m \rangle$; c) fundamental rms amplitude at the 0.7 $\langle U_m \rangle$ points.

effects on free jets. In the latter case, it is known that large-amplitude excitation at frequencies much lower than the initial shear-layer instability frequency can profoundly excite the jet. The lower-frequency disturbance is maximally amplified by the shear layer downstream and apparently corresponds to the linear instability of the thicker shear layer there.[15] The fundamental amplitude in that case grows to a maximum shortly downstream of that location. It was thought that a similar effect might be taking place in the present flow. However, the data of Fig. 9c bears evidence to the contrary. Clearly, the amplification is taking place right around the leading edge rather than at a location farther downstream.

Also shown in Fig. 9(c) are $\langle u_f' \rangle$ data for the lower shear layer emanating from the trailing edge. Obviously, the lower shear layer has also been excited similarly as compared to the upper one. However, it is reasonable to believe that this has very little effect on the airfoil performance. Figure 9a clearly indicates that the mean flowfield is affected primarily in the upper shear layer causing the observed improvement in the airfoil performance.

Traces of the velocity signal at different streamwise locations are shown in Fig. 10. At each x', the data represent the transverse location where $\langle u_f' \rangle$ is approximately the maximum; the vertical scale for each trace is the same. As the perturbation negotiates the leading edge, the amplitude grows rapidly. At $x'/c = -0.05$, the fundamental $\langle u_f' \rangle$ is less than 2% of U_∞ but becomes nearly 40% at $x'/c = 0.03$. Note that at the reference location ($x'/c \approx -0.4c$), the transverse component of the fundamental, $v_f'/U_\infty = 1.5\%$, but the streamwise component, u_f'/U_∞ is nearly zero. Downstream of the leading edge, u_f' becomes large and v_f' must be nearly zero due to the proximity of the wall. ($\langle u_f' \rangle$ should nearly equal u_f' at most measurement locations.) Turbulent breakdown is apparent at $x'/c = 0.07$, which is commensurate with the data of Fig. 9. The velocity traces in Fig. 10 also indicate an absence of significant subharmonic(s) in the signals. This was clearer from u' spectra at various locations (not shown) that were measured to obtain the transverse and streamwise profiles of Figs. 8 and 9c. In both Refs. 5 and 13, evidence of vortex pairing was reported. In an experiment on the effect of excitation on the flow over a backward facing step,[16] significant pairing activity was also noted. The excitation amplitude in the present experiment is apparently much larger, and there is no clear evidence of pairing that would be accompanied by the generation of a subharmonic. It is possible that the large

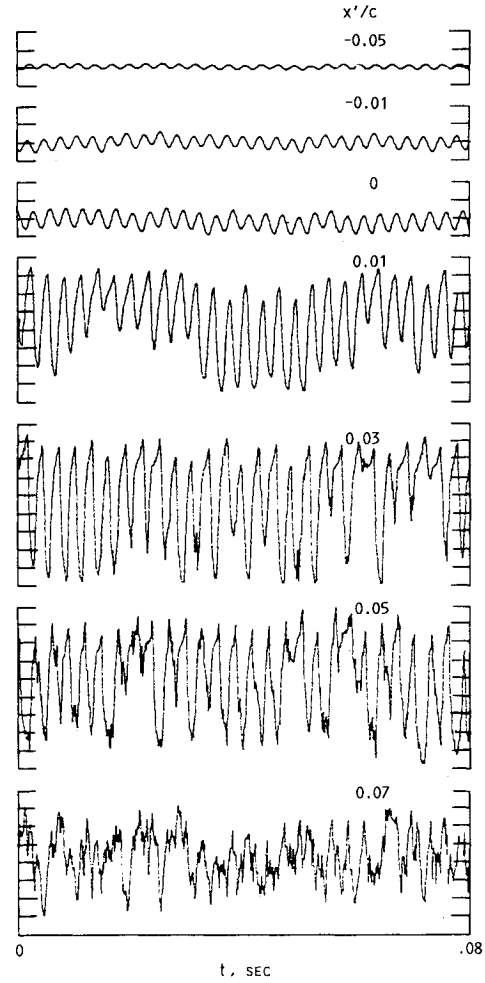

Fig. 10 Time traces of $\langle u \rangle$ signal at indicated x'/c locations for the excitation case of Fig. 7. At each x', the probe was located to approximately capture largest fluctuation amplitude.

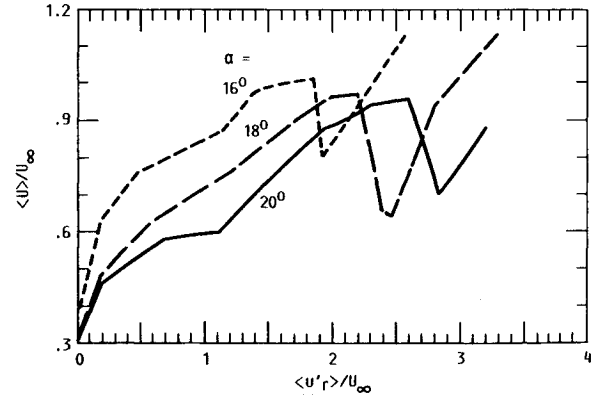

Fig. 11 Mean velocity at $x'/c = 0.3$ and about $0.1c$ above the surface, as a function of excitation amplitude.

amplitude excitation generates large-size vortices and the proximity of the wall inhibits lateral displacement of alternate vortices that must precede the vortex pairing process.

C. Saturation in Lift Enhancement

Referring back to Fig. 3, recall that for the low α cases the C_l variation indicated a saturation and subsequent breakdown with increasing excitation amplitude. This behavior was investigated further. The hot wire was placed at $x'/c = 0.3$ at a transverse location where the mean velocity was approximately 0.3 U_∞. As the excitation was initiated, the separated shear layer was drawn closer to the surface, which manifested in an increase in the mean velocity as measured by the hot wire. The variation of the mean velocity, read at the fixed location, with $\langle u_r' \rangle$ is shown in Fig. 11. Note that the variations for the three α cases are commensurate with the data trends shown in Fig. 3. The breakdowns in the curves occur at about the same amplitude levels. These data independently confirm the trend observed in Fig. 3.

The airfoil was now held at $\alpha = 18$ deg and the flowfields before and after the breakdown (at amplitudes of 1.8 and 2.4%, respectively) were investigated. When switched from one to the other amplitude, anomalies in the operation of the facility, such as variations in α and U_∞, were carefully monitored to ensure that they remained unchanged. The spectra of the reference velocity signals u_r' and v_r' indicated pure tone excitation at both amplitudes with higher harmonics no larger than 2% of the fundamental.[12] Thus, the breakdown at the higher amplitude was not due to some sort of distortion in the imparted excitation.

For the two amplitudes, the loci of the 0.7 $\langle U_m \rangle$ points (as in Fig. 9a), as well as the corresponding $\langle u_f' \rangle$ were measured. These data are shown in Fig. 12. Not unexpectedly, for the 2.4% amplitude, $\langle u_f' \rangle$ grows to a higher level and stays high everywhere relative to the other case. The $y_{0.7}$ data clearly show that the flow opens up downstream (for $x'/c \gtrsim 0.15$), i.e., the transverse extent of the separated region becomes larger, at the higher amplitude reconciling with the observed reduction in the lift. Near the leading edge, the $y_{0.7}$ data indicate the existence of a separation bubble which is more prominent for the lower-amplitude case. At 2.4% amplitude, the bubble appears to break open. Why the bubble breaks open at the higher amplitude is much too complex to address and remains unknown at this time. But it is clear that this somewhat abrupt change in the bubble characteristic is accompanied by the flow divergence downstream which results in the observed decrease in the lift. Note that even though the lift decreases at the higher amplitude it is still much higher than the corresponding lift for the unexcited flow.

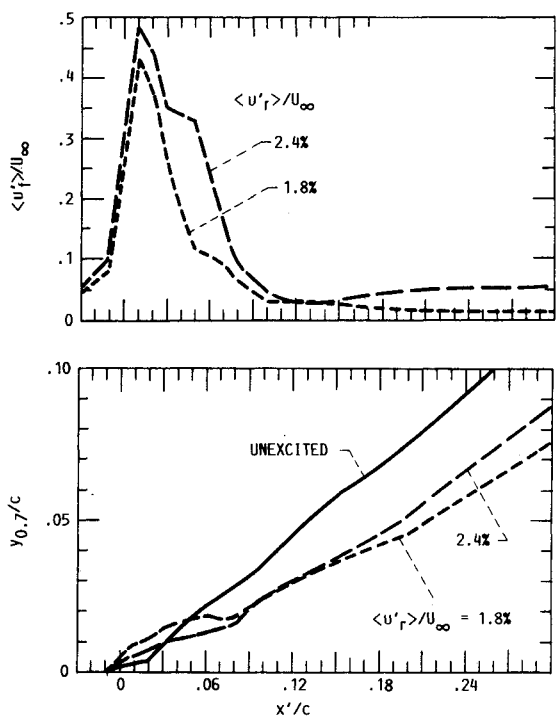

Fig. 12 $\langle u_f' \rangle$ and the loci of 0.7 $\langle U_m \rangle$ for two excitation amplitudes. Same flow as in Figs. 7 and 9.

IV. Concluding Remarks

Experimental results on the effect of acoustic excitation on poststalled flows at large α are summarized in this paper. It is shown that as the amplitude of excitation is increased, a large increase in the lift is achieved but the optimum effect shifts progressively to a lower Strouhal number. The Strouhal number yielding the optimum effect can be orders of magnitude lower than that corresponding to the linear, inviscid instability of the separated shear layer.

A similar observation was made in a relevant experimental study of the separation bubble over the blunt end of a cylinder placed parallel to the flow.[13] The excitation that resulted in a smaller bubble with accompanying reduction in drag, occurred at a frequency that was much lower than the Kelvin-Helmholtz instability frequency of the separated shear layer. It was hypothesized that a separation bubble is characterized by a shedding-type instability whose frequency f_s scales with the bubble height h and the freestream speed outside the bubble U_m such that $f_s h/U_m \approx 0.08$. The phenomenon was thought to be similar to vortex shedding from a bluff body, but due to the presence of the wall the interaction was with the image vortices, and thus, the nondimensional frequency was roughly one-half of that observed in the normal bluff body shedding. The data indicated that the optimum excitation effect took place when the nondimensional frequency was two to four times higher than the value noted earlier. The present results may be reviewed in this light. Referring back to the velocity profile at $x'/c = 0.03$ in Fig. 7 ($h \approx 3$ mm, $U_m \approx 1.6$ U_∞), a nondimensional value of about 0.08 is obtained for the effective frequency. This value, of course, is subjective and should vary depending on the amplitude and the measurement location but is interestingly close to the value of the so-called shedding instability frequency. A separation bubble oscillation has been reported by others also (e.g., Ref. 14). However, the concept of an associated instability and its role in the excitation process deserves further investigation in the future.

The flowfield data of the present study show that the imposed perturbation is amplified shortly downstream of the leading edge where it attains a very high level. But farther downstream, the flow becomes turbulent and the fundamental at the excitation frequency is hardly detectable beyond the 7% chord location. At α values close to static stall condition, the trend of increasing lift with increasing excitation amplitude undergoes an abrupt breakdown. This behavior is found to be associated with a separation bubble, occurring under the excitation, near the leading edge. At high excitation amplitudes, the bubble is broken up or reduced in size resulting in the observed breakdown in the lift.

The appearance of the separation bubble, which is characteristic of low R_c flows, raises the question if the inferences made from the present experiment will be applicable at higher R_c. As discussed in Sec. I, one may classify the poststalled flows into two broad categories: 1) at low R_c, the separated shear layer is initially laminar, and 2) at high R_c, the separating shear layer is already turbulent. $R_c \approx 5 \times 10^5$ may be considered as the borderline,[17] although this depends largely on the airfoil shape and the freestream conditions. The present experiment as well as most of the ones listed in Table 1 deal with class 1 flows. Certainly, the separation bubble must involve an initially laminar shear layer and, thus, the observed

breakdown in the lift must be characteristic of only the class 1 flows. However, the experiment of Ref. 2 involved a class 2 flow, as a boundary-layer trip was used near the leading edge. First, this proves that class 2 flows can also be excited to improve airfoil performance. This should not be surprising as there is ample proof that excitation can significantly influence an initially fully turbulent shear layer.[16,18] Second, for the initially turbulent shear layer in class 2 flows, only high amplitude excitation may be expected to be effective. Under the high amplitude excitation, according to the present results, the most pronounced effect may be expected to occur when the Strouhal number is low with a value on the order of unity.

References

[1]Collins, F. G., and Zelenevitz, J., "Influence of Sound upon Separated Flow over Wings," *AIAA Journal,* Vol. 13, No. 3, 1975, pp. 408–410.

[2]Ahuja, K. K., and Burrin, R. H., "Control of Flow Separation by Sound," AIAA Paper 84-2298, Oct. 1984.

[3]Marchman, J. F., Sumantran, V., and Schaefer, C. G., "Acoustic and Turbulence Influences on Stall Hysteresis," *AIAA Journal,* Vol. 25, No. 1, 1987, pp. 50–51.

[4]Mueller, T. J., and Batill, S. M., "Experimental Studies of Separation on a Two-Dimensional Airfoil at Low Reynolds Numbers," *AIAA Journal,* Vol. 20, No. 4, 1982, pp. 457–463.

[5]Nishioka, M., Asai, S., and Yoshida, S., "Control of Flow Separation by Acoustic Excitation," *AIAA Journal,* Vol. 28, No. 11, 1990, pp. 1909–1915.

[6]Huang, L. S., Maestrello, L., and Bryant, T. D., "Separation Control over an Airfoil at High Angles of Attack by Sound Emanating from the Surface," AIAA Paper 87-1261, 1987.

[7]Hsiao, F., Liu, C., Shyu, J., and Wang, M., "Control of Wall Separated Flow by Internal Acoustic Excitation," AIAA Paper 89-0974, Oct. 1989.

[8]Neuburger, D., and Wygnanski, I., "The Use of a Vibrating Ribbon to Delay Separation on Two-Dimensional Airfoils: Some Preliminary Observations," Workshop on Unsteady Separated Flow, U.S. Air Force Academy, Colorado Springs, CO, July 1987 (private communication).

[9]Bar-Sever, A., "Separation Control on an Airfoil by Periodic Forcing," *AIAA Journal,* Vol. 27, No. 6, 1989, pp. 820–821.

[10]Zaman, K. B. M. Q., Bar-Sever, A., and Mangalam, S. M., "Effect of Acoustic Excitation on the Flow over a Low-*Re* Airfoil," *Journal of Fluid Mechanics,* Vol. 182, 1987, pp. 127–148.

[11]Zaman, K. B. M. Q., McKinzie, D. J., and Rumsey, C. L., "A Natural Low Frequency Oscillation of the Flow over an Airfoil Near Stalling Conditions," *Journal of Fluid Mechanics,* Vol. 202, 1989.

[12]Zaman, K. B. M. Q., and McKinzie, D. J., "Control of Laminar Separation over Airfoils by Acoustic Excitation," *AIAA Journal,* Vol. 29, No. 7, 1991, pp. 1075–1983.

[13]Sigurdson, L. W., and Roshko, A., "Controlled Unsteady Excitation of a Reattaching Flow,"AIAA Paper 85-0552, 1985.

[14]Simpson, R. L., "Two-Dimensional Turbulent Separated Flow," AGARD AG-287, Vol. 1, June 1985.

[15]Petersen, R. A., and Samet, M. M., "On the Preferred Mode of Jet Instability," *Journal of Fluid Mechanics,* Vol. 194, 1988, pp. 153–173.

[16]Roos, F. W., and Kegelman, J. T., "Structure and Control of Flow over a Backward-Facing Step," *Forum on Unsteady Flow Separation,* edited by K. N. Ghia, American Society of Mechanical Engineers, New York, 1987, pp. 215–223.

[17]Mueller, T. J., "Low Reynolds Number Vehicles," AGARD AG-288, Feb. 1985.

[18]Crow, S. C., and Champagne, F. H., "Orderly Structures in Jet Turbulence," *Journal of Fluid Mechanics,* Vol. 48, pp. 547–591.